

# Phase-Based Image Analysis of 3D Seismic Data

**Peter Kovesi**<sup>1</sup>

*peter.kovesi@uwa.edu.au*

**Ben Richardson**<sup>1,2</sup>

*richab02@student.uwa.edu.au*

**Eun-Jung Holden**<sup>1,2</sup>

*eun-jung.holden@uwa.edu.au*

**Jeffrey Shragge**<sup>2</sup>

*jeffrey.shragge@uwa.edu.au*

<sup>1</sup>*Centre for Exploration Targeting, The University of Western Australia, WA 6009, Australia*

<sup>2</sup>*Centre for Petroleum Geoscience and CO<sub>2</sub> Sequestration, The University of Western Australia, WA 6009, Australia*

## SUMMARY

Automated image analysis techniques can be effectively used to detect discontinuities (e.g. faults, pinchouts, channels, etc.) within seismic data in a non-subjective manner. Conventional image processing techniques, such as the coherency cube, typically locate discontinuities by finding regions of sharp intensity shifts and are thereby sensitive to contrast variations and noise. Here, we present a phase-based technique that offers contrast-invariant and noise-robust feature characterisation through local phase and orientation information.

Phase congruency is an edge-detection algorithm that differs from traditional approaches by defining edges as points where the Fourier components of a signal are maximally in phase. Applying 2D phase congruency to horizontal time slices extracted from a 3D seismic volume is problematic, though, because horizons are rarely parallel to horizontal time slices, causing horizon boundaries to appear artificially discontinuous. To better detect 3D seismic discontinuities, we extend phase congruency to a 3D algorithm using conic spread filters that provides a localised, multi-scale and dip-independent feature detector.

Preliminary results show that 3D phase congruency is capable of detecting velocity anomalies, but has some limitations in identifying fault boundaries in seismic data. However, it can provide an increased level of feature detail over conventional coherency cube processing. More importantly, these results indicate the potential for using multidimensional phase-based algorithms in 3D/4D seismic processing and imaging workflows, with particular applications in image denoising, image registration, feature detection, and velocity model verification.

**Key words:** phase congruency, seismic processing, 3D feature detection, automated interpretation.

Phase congruency is an edge detection algorithm that differs from traditional approaches by defining edges as points where the Fourier components of a signal are maximally in phase (Morrone and Owens, 1987; Morrone and Burr 1988). In a study by Russell et al. (2010), 2D phase congruency was applied to horizontal time slices within a 3D volume in an attempt to enhance seismic discontinuities. However, seismic discontinuities are 3D features and require a 3D approach to be properly resolved. Also, as horizons are rarely parallel to horizontal time slices, horizons appear discontinuous. To address these issues we have developed a full 3D implementation of phase congruency and compared its performance with other standard techniques on seismic data.

## PHASE CONGRUENCY

Traditionally, image feature detectors have been developed to identify points of high gradient in the signal. However, it has been shown that points of high gradient may only represent a limited subset of the features of interest (Kovesi 2002). An alternative model of feature detection is that points of interest are perceived at locations of phase congruency (Morrone and Owens, 1987; Morrone and Burr, 1988). Figure 1 illustrates the congruence of phase that occurs at the point of a step in a square waveform and at the peaks of a triangular waveform. Depending on the angle at which congruence of phase occurs a wide range of different feature types can be produced. Thus, this model of feature perception allows a broad range of feature types to be detected within the one framework.

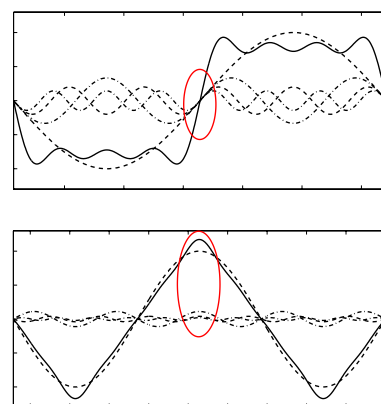


**Figure 1.** Congruence of phase at the point of the step in a Fourier series forming a square wave (top panel), and at the peaks of a triangular wave (bottom panel).

The measurement of phase congruency at a point in a signal can be seen geometrically in Figure 2. The local, complex valued, Fourier components at a location  $x$  in the signal will have an amplitude  $A_n(x)$  and phase angle  $\phi_n(x)$ . Figure 2

plots these local Fourier components as complex vectors adding head to tail. The magnitude of the vector from the origin to the end point is the *Local Energy*  $|E(x)|$ . The measure of phase congruency devised by Morrone and Owens (1987) is

$$PC(x) = \frac{|E(x)|}{\sum A_n(x)}$$

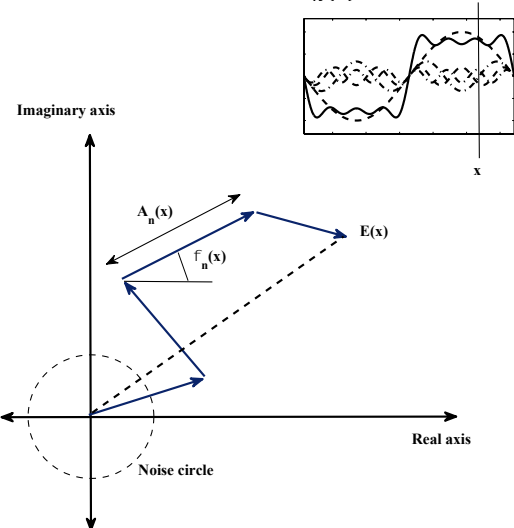


**Figure 2.** Polar diagram of local Fourier components at a location  $x$  in the signal, plotted head to tail, illustrating the computation of phase congruency.

Under this definition phase congruency is the ratio of  $|E(x)|$  to the overall path length taken by the local Fourier components in reaching the end point. At a point of phase congruency all the phase vectors will be aligned and the ratio of  $|E(x)|$  to  $\sum A_n(x)$  will be one. If there is no coherence of phase this ratio falls to a minimum of zero. Thus, phase congruency is a dimensionless quantity that is unaffected by signal offsets or contrast. This makes it a useful tool for analysing the wide range of values that may be present in geophysical signals.

However, in its basic form, this measure of phase congruency is sensitive to noise and is also degenerate if there is only one frequency component present in the signal. Accordingly this measure of phase congruency has been further developed by Kovesi (1999) to incorporate a more sensitive measure of phase deviation and a weighting for the spread of frequencies present in the signal. To account for noise a threshold is set defining the magnitude of local energy in the signal that can be expected to arise naturally from the noise in the signal, this is indicated by the noise circle shown in Figure 2. This threshold can be set manually but can also be estimated automatically from the signal itself (Kovesi, 1999). Then, when computing phase congruency, only the amount that  $|E(x)|$  exceeds the radius of the noise circle is considered. This noise compensation scheme bears some similarities to wavelet shrinkage denoising (Donoho, 1995).

The description of phase congruency outlined above only applies to 1D signals. In 2D we implement phase congruency by convolving the signal with a series of oriented 2D complex valued log-Gabor filters over a range of different centre frequencies. From this we obtain local phase and amplitude data at a number of scales and over a series of orientations (Field, 1987; Kovesi, 1999). Typically, filters at three to four scales over six orientations are used. For efficiency the

convolutions of the signal with the log-Gabor filters are performed in the Fourier domain. The transfer functions of the filters form a rosette around the origin (Figure 3). Phase congruency is then evaluated in each of the orientations independently and a covariance matrix relating phase congruency in the  $x$  and  $y$  directions is formed. The maximum eigenvalue provides an overall measure of phase congruency, and the corresponding eigenvector indicates the local orientation of the feature in the signal. The minimum eigenvalue of the covariance matrix is also useful in that it provides an indication of the isotropy of the feature. For further details of the implementation of phase congruency in 2D see Kovesi (1999, 2000, 2003).

To extend the computation of phase congruency to 3D we adopt a similar approach. The main consideration is to obtain good filter coverage over all orientations in 3D while using a minimal number of filters in order to maintain a tractable computational load. We have chosen to use the surface normals of the faces of an icosahedron to define the 3D filter orientations, as shown in Figure 3 (Richardson, 2010). This results in ten filter orientations. While more orientations might be preferable to obtain a more complete filter coverage over all 3D orientations this appears to be a reasonable compromise that allows computation in an acceptable amount of time.

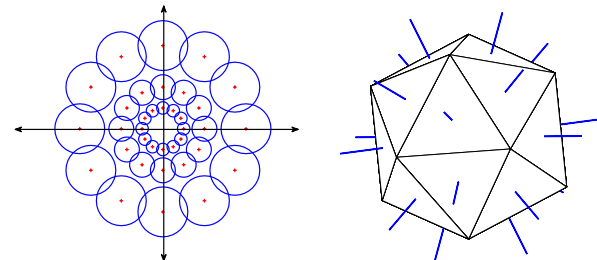


**Figure 3.** In 2D the transfer functions of the log-Gabor filters form a rosette in the 2D frequency plane (left). This example shows filters over three scales and six orientations. A similar approach is used to define the filters in 3D using the surface normals of the faces of an icosahedron to define the filter orientations (right).

## RESULTS

We applied the phase congruency analysis to a time-migrated seismic data acquired in Western Australia's Carnarvon Basin. The geology in this survey region is noted for significant faulting and localized near-surface velocity anomalies. We extracted two 128x128x128 subcubes from the full data volume for testing our 3D phase-congruency algorithm.

We conducted two experiments comparing the effectiveness of using the coherency cube, and 2D and 3D phase congruency at resolving two different features noted in the data. The first test involved a high-amplitude reflector feature interpreted to be a mud volcano, which appears as a (poorly resolved) velocity anomaly in Figures 4 and 5. The second experiment involved trying to resolve faults in an area of complex geology, shown in Figures 6 and 7.

We used filters over four scales with a minimum wavelength of three pixels increasing by a factor of two at each scale. For 3D phase congruency we used ten filter orientations, as defined by the faces of an icosahedron. The 2D phase congruency results were obtained using six orientations. The

coherency volume calculations were based on a 3x3x3 volume window.

Figures 4 and 5 show that 3D phase congruency is effective in detecting velocity anomalies caused by bright reflectors. In comparison to other methods, 3D phase congruency provides significantly more detail on the resulting seismic disturbances underneath while 2D phase congruency produces a large number of anomalous features caused by the separation of horizons on each slice. Figures 6 and 7 show that phase congruency is capable of detecting fault boundaries, but it lacks the clarity and cleanliness of the coherency cube response. Phase congruency detects the step edges caused by the phase shift across the fault and, while this result has applications in image matching and velocity modelling, it lacks a clear and simple representation of the 3D fault structure within the image.

## CONCLUSIONS

While more investigation into the behaviour of phase congruency at faults is needed, it appears that faults are mainly characterised by a local change in signal orientation rather than a sharp change in signal strength. Thus, phase congruency on its own may not be the optimal way to detect faults. Future work will focus on detecting local-phase discontinuities to provide better measures for feature enhancement. However, where 3D phase congruency may prove most useful is in the identification of local orientations within the data volume, and the identification of orientation discontinuities. It is this area that we plan to develop in the future. Orientation data provides important geological indications. The use of 3D phase congruency provides a framework from which orientation information can be obtained regardless of the data volume coordinate system. In comparison, orientation data calculated with 2D phase congruency is confined to the analysis plane and the coherency cube provides no easy access to local orientation.

## REFERENCES

- Donoho, D.L., 1995, Denoising via soft thresholding: IEEE Transactions on Information Theory, **41**, 613–627.
- Field, D.J., 1987, Relations Between the Statistics of Natural Images and the Responses of Cortical Cells: Journal of the Optical Society of America A, **4**(12), 2379-2394.
- Kovesi, P.D., 1999, Image Features From Phase Congruency: Videre: A Journal of Computer Vision Research, **1**(3), 1-26.
- Kovesi, P.D., 2000, MATLAB and Octave Functions for Computer Vision and Image Processing: Centre for Exploration Targeting, The University of Western Australia. <http://www.csse.uwa.edu.au/~pk/research/matlabfns/>
- Kovesi, P.D., 2002, Edges are not Just Steps: Proceedings of ACCV2002 The Fifth Asian Conference on Computer Vision, 822-827.
- Kovesi, P.D., 2003, Phase Congruency Detects Corners and Edges: Proceedings of The Australian Pattern Recognition Society Conference: DICTA 2003, 309-318.
- Morrone, M.C. and Owens, R.A., 1987, Feature Detection from Local Energy: Pattern Recognition Letters, **6**, 303-313.

Morrone, M.C. and Burr, D.C., 1988, Feature Detection in Human Vision: A Phase-Dependent Energy Model: Proceedings of the Royal Society, London B, **235**, 221-245.

Richardson, B.J., 2010, Development of a 3D Phase Congruency Program for the Study of Articular Cartilage: Hons. Thesis, The University of Western Australia.

Russell, B., Hampson, D. and Logel, J., 2010, Applying the Phase Congruency Algorithm to Seismic Data Slices: A Carbonate Case Study: First Break, **28**, 84-90.

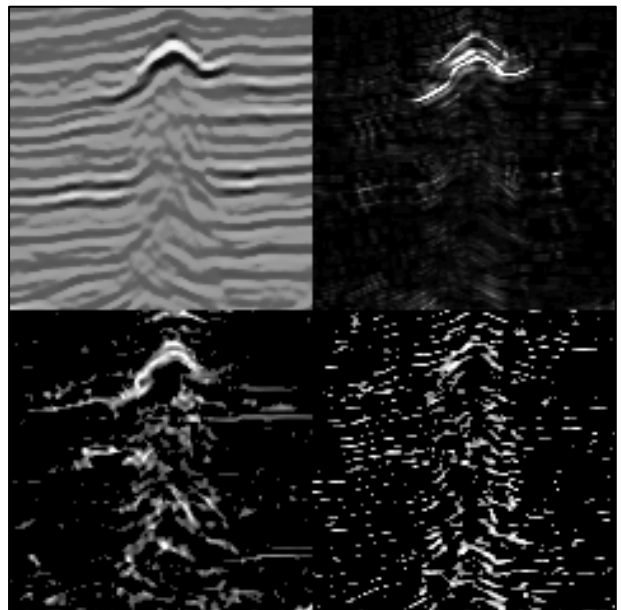


Figure 4: Vertical cross-section of the velocity anomaly test image (top left), coherency cube (top right), maximum moment of 3D phase congruency (bottom left), 2D phase congruency (bottom right).

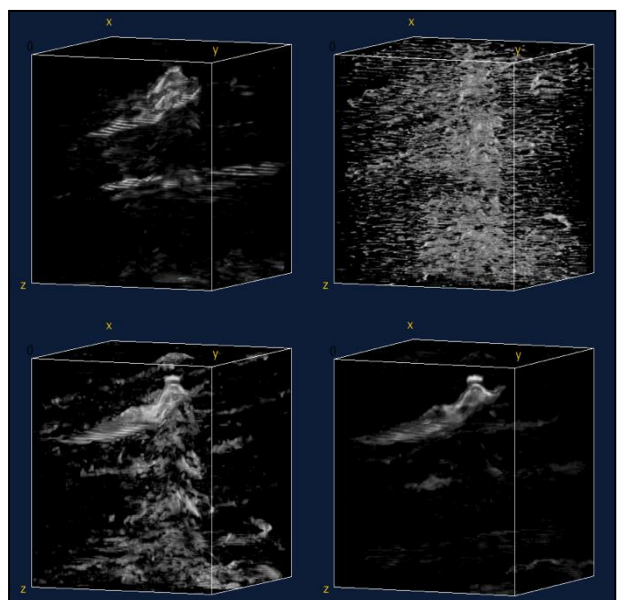


Figure 5. 3D visualisation of the response from the coherency cube (top left), 2D phase congruency (top right), and the maximum and minimum moments of 3D phase congruency (bottom left and right, respectively) for the velocity anomaly.

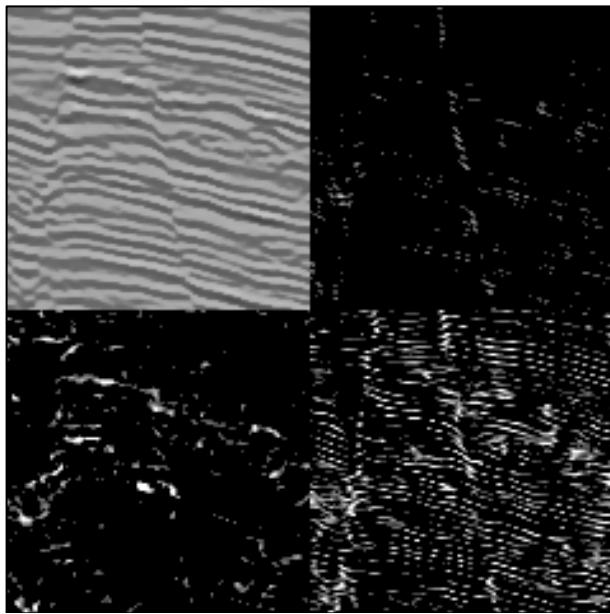


Figure 6: Vertical cross-section of the fault test image (top left), coherency cube (top right), maximum moment of 3D phase congruency (bottom left), 2D phase congruency (bottom right).

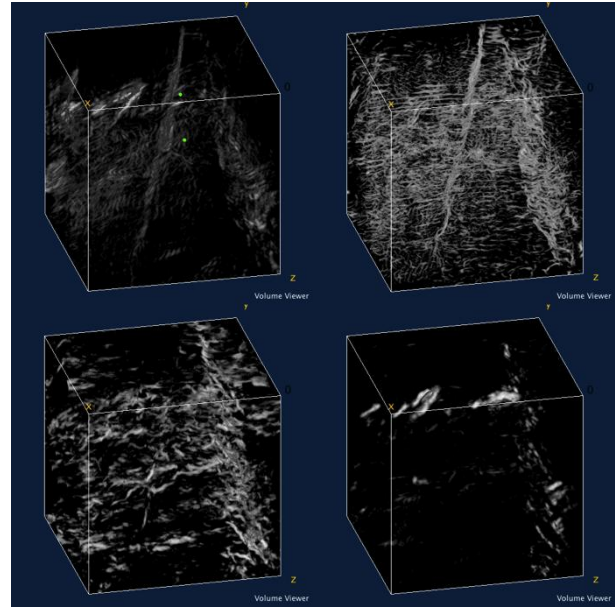


Figure 7. 3D visualisation of the response from the coherency cube (top left), 2D phase congruency (top right), and the maximum and minimum moments of 3D phase congruency (bottom left and right respectively) for the fault test image.